

Applying Different Normalisation Models to Improve Core Flow Inversion

1. Introduction

The Earth's magnetic field is generated by fluid motion of liquid iron in the outer core. Flows at the top of the outer core are believed to be responsible for the secular variation (SV) observed at the surface of the Earth. Modelling of this flow is open to considerable ambiguity, though methods adopting different physical assumptions do lead to similar flow velocity regimes.

We investigate the use of different 'best-fit' or 'minimisation' methods in core flow modelling based on past records of SV. We use a method for directly inverting the observed secular variation from permanent observatories, rather than through the use of spherical harmonic models. We have tested iterative one-norm minimisation models and find that they better describe the secular variation than the current two-norm models using the steady flow assumption. Here we present the preliminary results of flows generated using the dataset (Figure 1) modelled by Wardinski (2005). We re-examine the hypothesis of whether flow at the top of the outer core can be assumed purely toroidal.

Data Collection and Processing

| Year | Co-latitude | Longitude | Height (km) | Obs. Code | dx/ut | Error (nT) | dy/ut | Error (nT) | dz/ut | Error (nT) |
|------|-------------|-----------|-------------|-----------|-------|------------|-------|------------|-------|------------|
| 1990 | 7.503 | 297.64 | 0.06 | ALE | 0 | 1 | 11 | 1 | -18 | 1 |
| 1990 | 9.263 | 58.05 | 0.02 | HIS | -34 | 1 | 1 | 1 | -30 | 1 |
| 1990 | 11.093 | 11.93 | 0.011 | NAL | -25 | 1 | 5 | 1 | -6 | 1 |
| 1990 | 12.283 | 104.28 | 0.01 | CCS | -33 | 1 | 5 | 1 | -50 | 1 |
| 1990 | 12.523 | 290.76 | 0.057 | THL | 21 | 1 | 2 | 1 | -51 | 1 |
| 1990 | 13 | 13.55 | 0.015 | HRV | -34 | 1 | 12 | 1 | 7 | 1 |
| 1990 | 13.685 | 240.63 | 0.04 | MBC | 26 | 1 | -15 | 1 | -58 | 1 |
| 1990 | 15.31 | 265.10 | 0.03 | RES | 35 | 1 | -2 | 1 | -65 | 1 |
| 1990 | 16.457 | 80.56 | 0.015 | DKW | -35 | 1 | 2 | 1 | -25 | 1 |
| 1990 | 18.417 | 129 | 0.04 | TKK | -27 | 1 | -2 | 1 | -30 | 1 |
| 1990 | 34.683 | 356.8 | 0.242 | ESK | 13 | 1 | 30 | 1 | 13 | 1 |

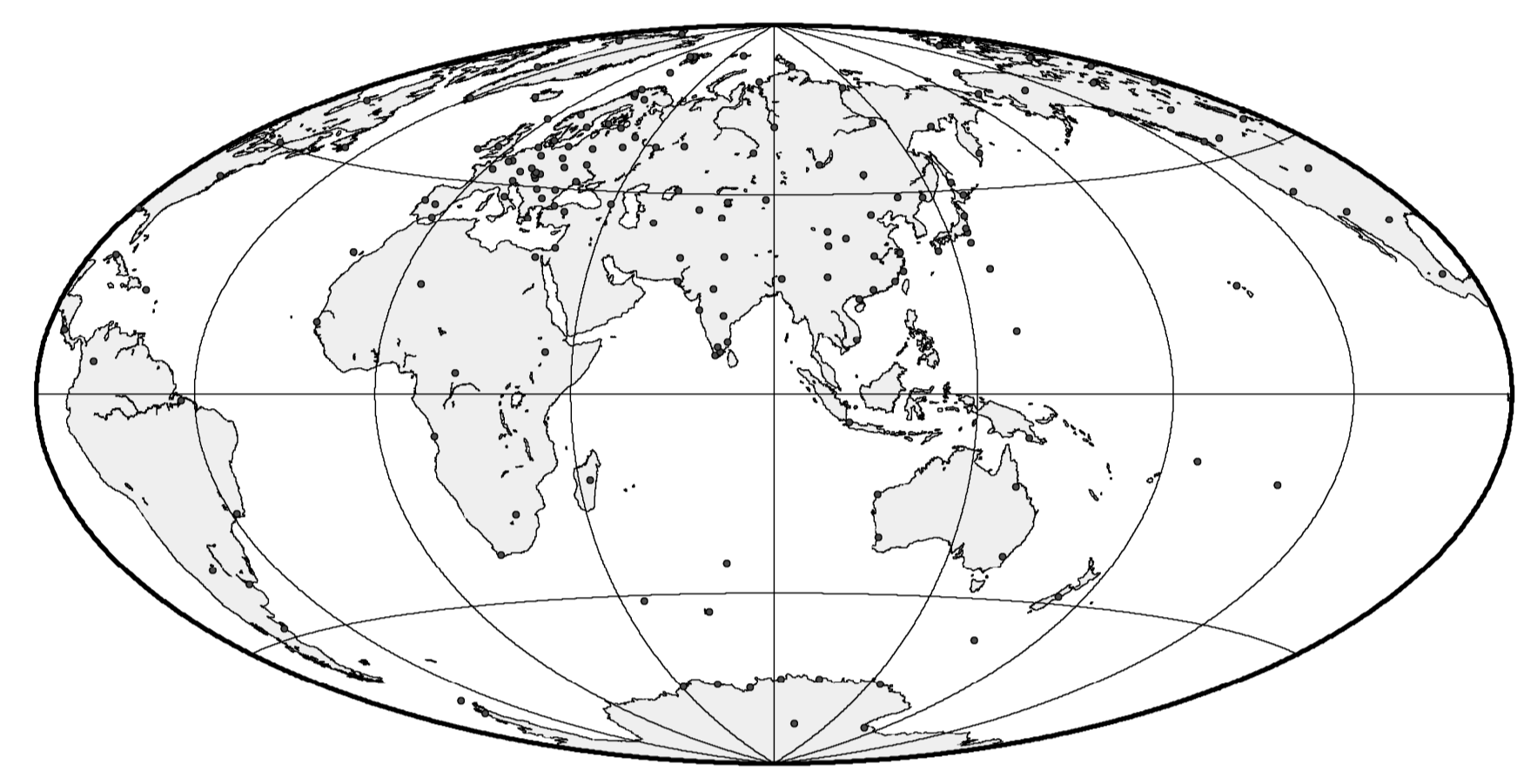
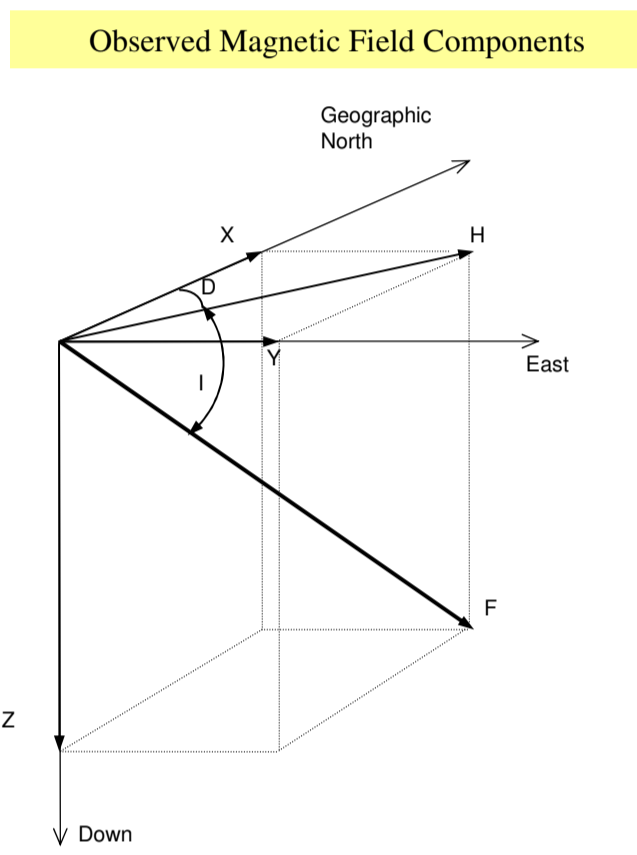


Figure 1: Secular Variation from 172 permanent observatories (red points) and an example of the SV of three components (\dot{X} , \dot{Y} , \dot{Z})

2. Method

It has been suggested that the use of a 1-norm measure of misfit of the model data to secular variation should be used to infer core fluid flow. It has previously been assumed that the noise within observations of the magnetic field has a Gaussian distribution. However, empirical evidence, from the main field, appears to show that the noise follows a Laplacian (double exponential) distribution [Walker and Jackson (2000)].

This motivates the use of a one-norm measure of misfit of weighted residual between observations and model estimates. The one-norm model solves the equation of the form:

$$(\mathbf{A}^T \mathbf{C}_e^T \mathbf{R} \mathbf{C}_e \mathbf{A} + \lambda \mathbf{D}) \mathbf{m}^{k+1} = \mathbf{A}^T \mathbf{C}_e^T \mathbf{R} \mathbf{C}_e \mathbf{d}$$

where there is a linear relation between the spherical harmonic coefficients of the flow and secular variation observations. \mathbf{A} is the equations of condition matrix, \mathbf{C}_e is diagonal with the inverse of the standard deviations along the diagonal, λ is the damping parameter, \mathbf{D} is the regularization matrix, and \mathbf{d} the data vector. \mathbf{m}^{k+1} is the $(k+1)$ th solution iteration. The solution is non-linear because the diagonal misfit matrix \mathbf{R} has elements $\sqrt{2}/|\epsilon_i|$, where ϵ_i is the normalised residual to the i th datum. In the two-norm model, \mathbf{R} becomes the identity matrix and only one iteration is required to solve the system. This is equivalent to the least-squares solution. The solution for the one-norm model typically converges after fifteen to twenty iterations (Figure 2). The parameter λ controls the smoothness of the solution.

The model assumes that the Secular Variation can be equated to the toroidal (\mathbf{t}) and poloidal (\mathbf{s}) coefficients of the flow through the Gaunt (\mathbf{G}) and Elsasser (\mathbf{E}) matrices. The observatory data (\mathbf{d}) are converted to spherical harmonic representations using the matrix \mathbf{Y} (see Figure 2). The model coefficients (\mathbf{m}) are calculated from input data (\mathbf{d}) using a stochastic inversion method (Figure 2).

Inferring Flow from SV

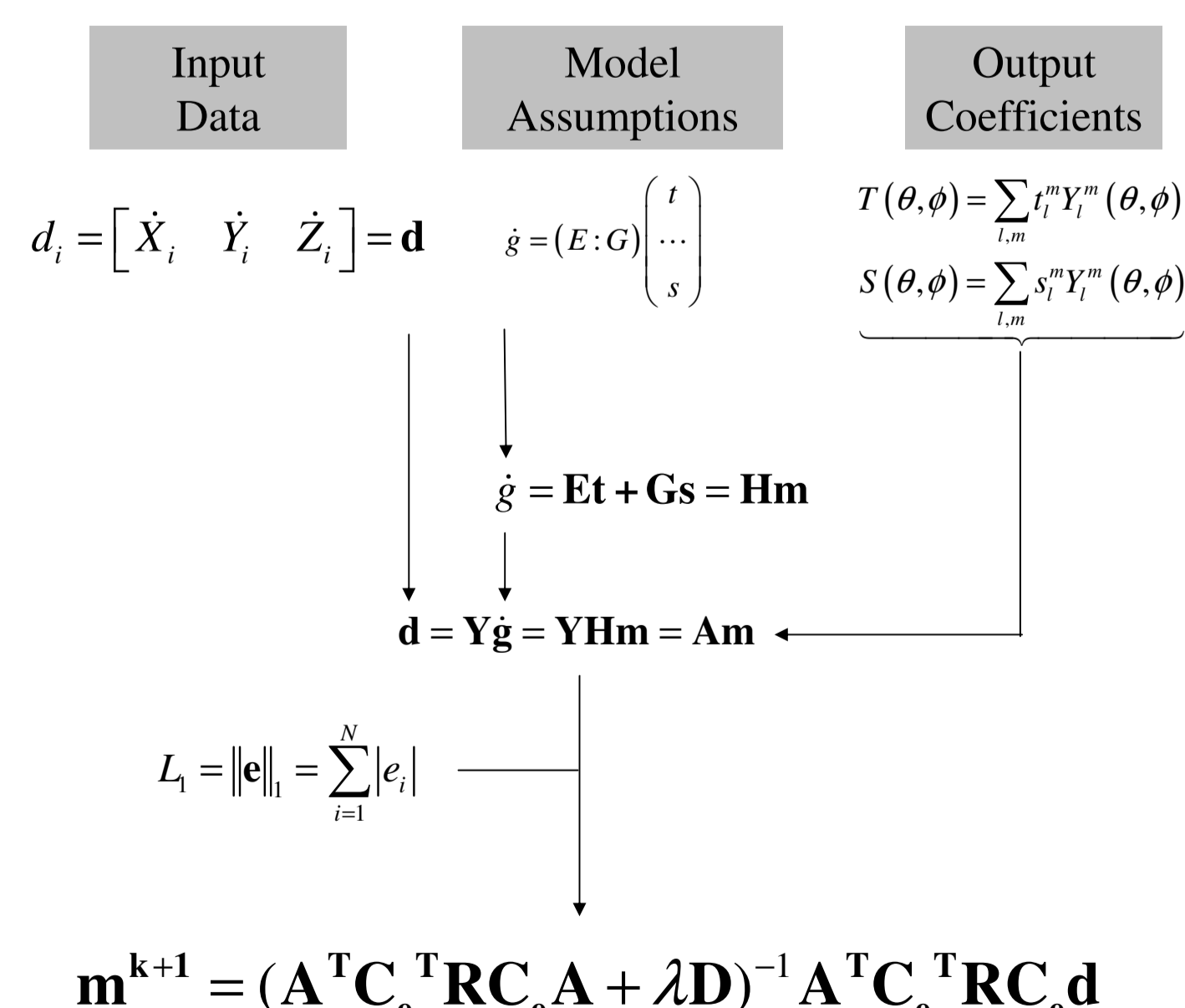
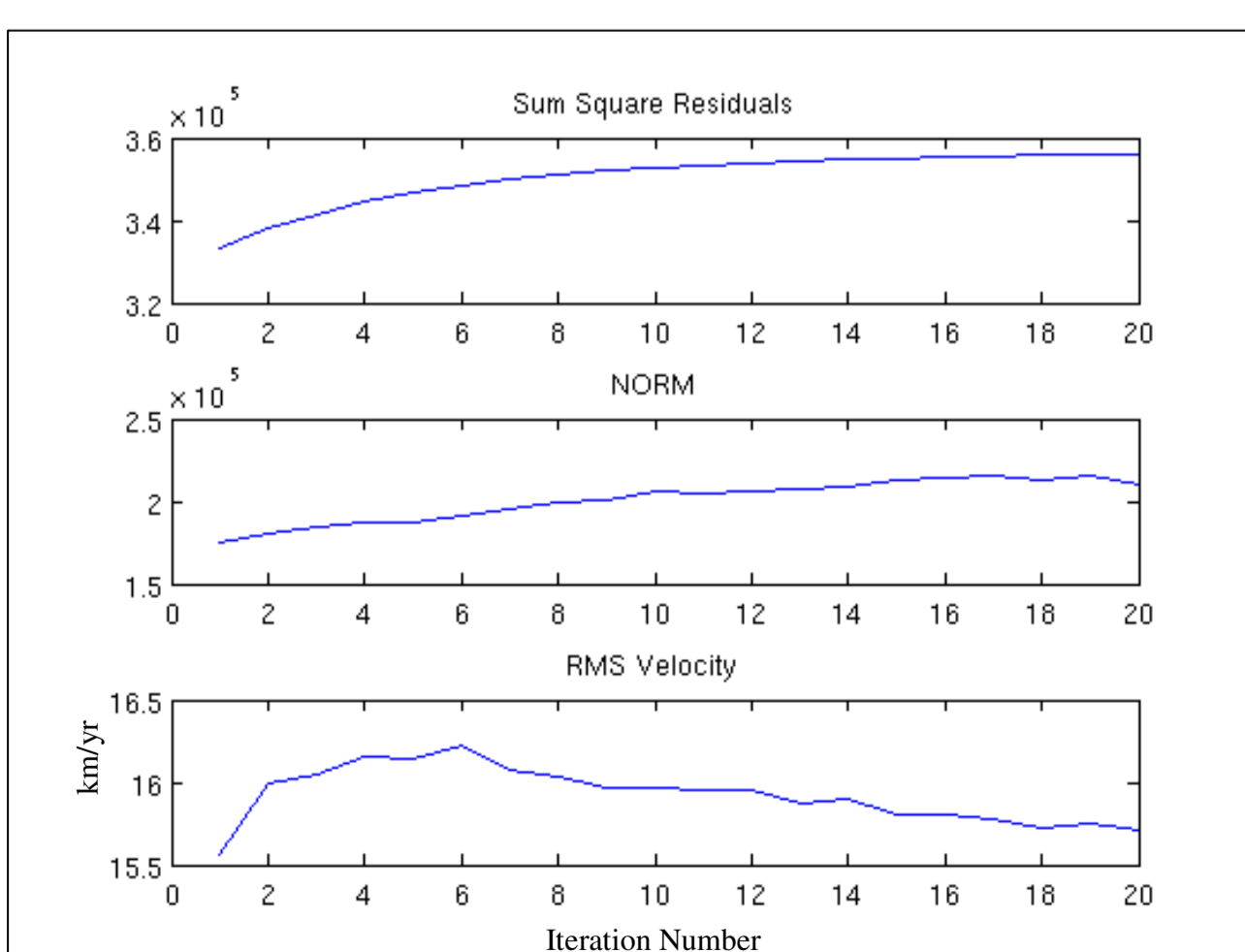


Figure 2: Iteration Metrics and Mathematical Model used to calculate core flow from Secular Variation.

3. Results

All flows have been calculated with the GUFM main field model with data from the 1990 epoch. Magnetic field observatory data have been adapted from Wardinski (2005). There are 172 data points (Figure 1) unevenly spaced across the globe. The flows are calculated up to degree and order 14. A steady flow has been assumed.

Figure 3 shows two-norm and one-norm solutions, varying the parameter λ . The residual error between observations and the model prediction ($\mathbf{d} - \mathbf{A}\mathbf{m}$) for each flow solution are plotted in the histograms. The expected (best-fit) Gaussian and Laplacian distributions are also shown on the histograms.

Flow Results from SV

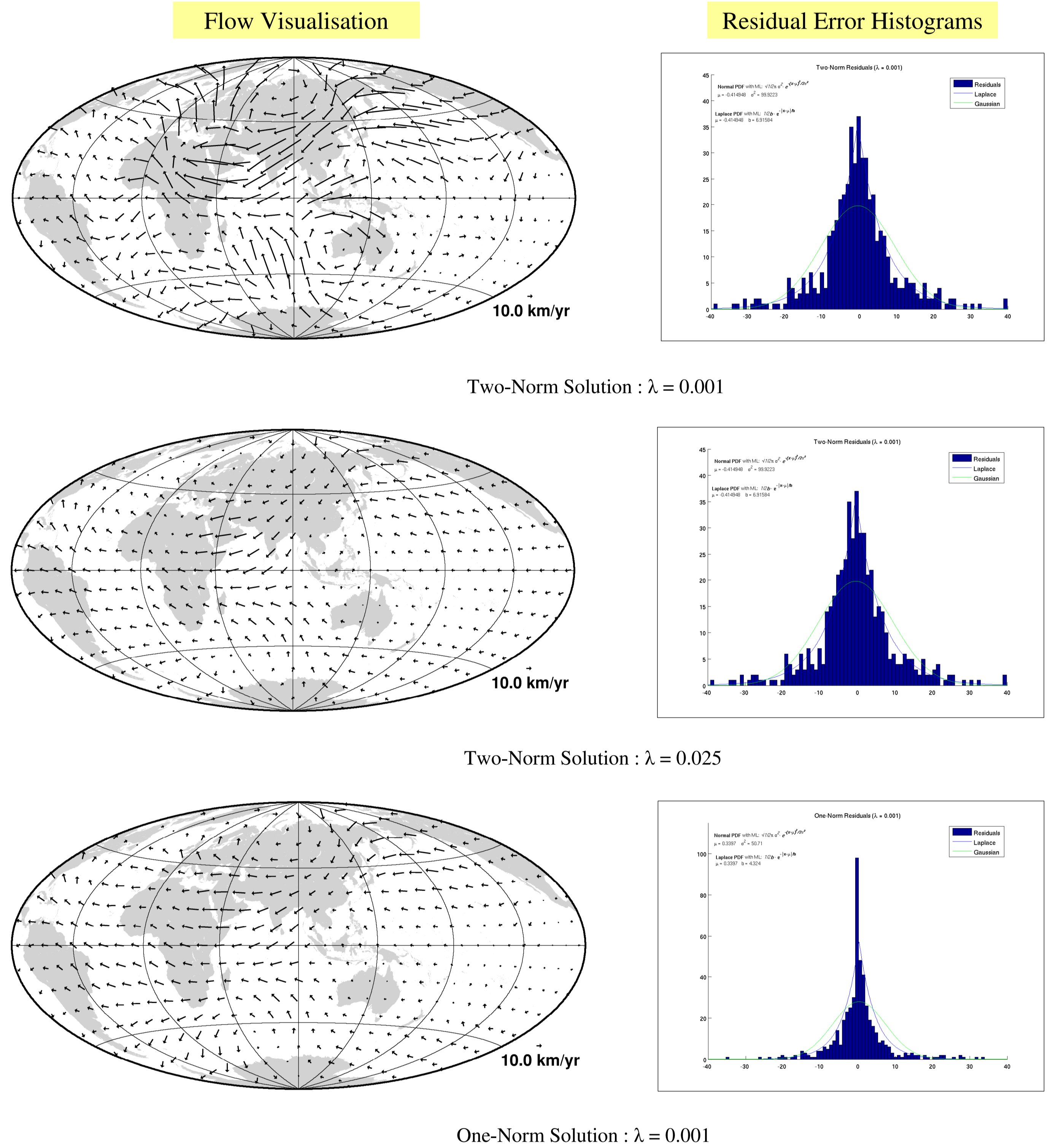


Figure 3: Core flow Models and Residual Error Histograms

4. Discussion / Future Work

The residual error histograms of the two-norm solutions clearly show that the Laplacian distribution better fits the mismatch between the input data and the model output. The use of a one-norm minimisation is thus justified by the improved fit of the model to the data, shown in the increased clustering of the residual errors about zero.

The summary statistics of the flows are shown in Table 1 (below). The toroidal and poloidal (also geostrophic and ageostrophic) contribution to each flow has been calculated. These indicate that most of the flow (~80%) resides in the toroidal coefficients. Further investigation of the fit of both toroidal only and poloidal only flows to the observatory data indicate that a significant poloidal flow does reduce the residual errors. The inference is that upwelling/downwelling of the fluid is likely at the Core-Mantle Boundary.

The next step is to incorporate data from satellite missions (CHAMP/Oersted) and global repeat stations to expand the global coverage of the data set. Recovery of the flow and projection of the flow forward in time for short periods are the main aims for the future, in order to produce a better prediction of the time evolution of the field over the short term (i.e. 5-10 years).

| Flow Type | Lambda | Flow Velocity (km / yr) | | | | | | |
|-----------|--------|-------------------------|----------|----------|-------------------|-------------|--------------|--------------------|
| | | Flow RMS | Toroidal | Poloidal | Ratio (Tor : Pol) | Geostrophic | Ageostrophic | Ratio (Geo : Ageo) |
| Two-Norm | 0.001 | 28.7 | 25.3 | 13.5 | 0.77 | 25.1 | 13.9 | 0.76 |
| Two-Norm | 0.025 | 12.7 | 11.6 | 5.4 | 0.81 | 11.1 | 6.1 | 0.75 |
| One-Norm | 0.001 | 14.1 | 12.9 | 5.4 | 0.85 | 12.6 | 6.2 | 0.81 |

Table 1: Velocity Components and Flow Ratios

5. References

- Walker, M. R., and Jackson, A., 2000. Robust modelling of the Earth's magnetic field, *Geophys. J. Int.*, 143, 799-808.
- Wardinski, I., 2005. PhD Thesis, Core Surface Flow Models from Decadal and Subdecadal Secular Variation of the Main Geomagnetic Field, GFZ Postdam.
- Whaler, K., Holme, R., Jackson, A., One-norm modelling of flow at the core-mantle boundary, Poster at SEDI Conference 2004
- Whaler, K., 1986. Geomagnetic evidence for fluid upwelling at the core-mantle boundary, *Geophys. J. R. Astr. Soc.*, 86, 563-588.